Proceedings of the 1997 IEEE
International Conference on Robotics and Automation
Albuquerque, New Mexico - April 1997

A Comparison of Real and Simulated Designs for Vibratory Parts Feeding

Dina R. Berkowitz* dberk@cs.berkeley.edu

John Canny* jfc@cs.berkeley.edu

Department of Electrical Engineering and Computer Science
University of California, Berkeley, CA 94720

Abstract

The design of industrial parts feeders is a long, trial-and-error process that can take months – even for the design of feeders that orient only one type of part. This paper describes the use of dynamic simulation to expedite the design and prototyping of parts feeders. We give probabilistic descriptions of vibratory parts feeding behavior, and we present a comparison between simulated design experiments and physical experiments done using a real industrial vibratory bowl feeder. Our findings show strong similarities between the results of the two types of experiments. We believe that dynamic simulation is a promising approach for expediting the parts feeder analysis and design process.

1 Introduction

Although the vibratory parts feeders used in industry to sort and orient parts are quite reliable, their design is time-consuming. This is largely due to the trial-and-error nature of the design process. We would like to use dynamic simulation to expedite the efficient and effective design of industrial parts feeders.

In our previous work, we described a tool to automatically generate, perform, and evaluate suites of feeder design experiments using dynamic simulation [1]. In that work and here we used Mirtich's impulse-based dynamic simulator, *Impulse* [11; 12].

Impulse uses a friction-based model to simulate the micro-collisions occurring between impacting bodies. A previous paper by Mirtich et al. gives results suggesting that Impulse can predict the dynamical interactions found in industrial parts feeding tasks [13]. Preliminary findings from our former work also suggest that dynamic simulation may be a promising approach for designing parts feeders. In this paper, we discuss results from our current parts feeding experiments.

The primary contribution of this paper is to compare the experimental results from designs we have simulated using dynamic simulation to those of an actual vibratory bowl. We show the accuracy of Impulse's simulation results by comparing them to an actual vibratory bowl feeder using real industrial parts.

*Financial support provided by National Science Foundation Grant #FD93-19412.

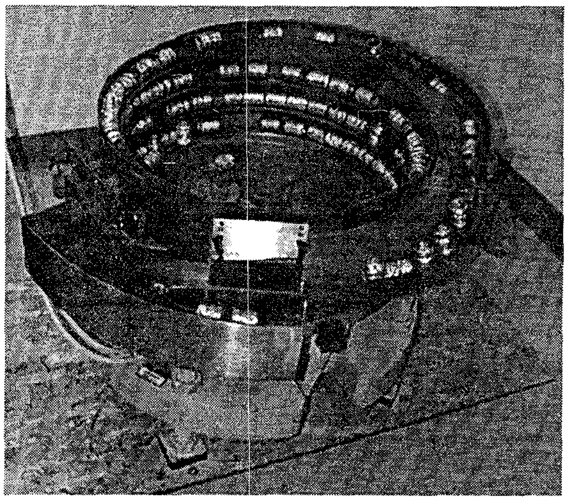

Figure 1: Our Vibromatic Company, Inc. vibratory bowl feeder for orienting industrial parts.

This paper also improves on previous work in two other ways. Formerly, we presented a Markov model to represent the behavior of parts feeders. Here we give examples from our recent experiments that demonstrate the use of this model. The paper also improves on previous work because it shows the use of vibrational parts feeding rather than simple gravitational feeding.

In the rest of the paper, we first present related work, our feeder model, and our experimental setup. Next we present probabilities for the behavior of some feeder designs that were generated using our tool. These allow us to give stochastic matrices that describe the probabilistic behaviors of feeder gates. We form a Markov model of the feeder using these matrices. We then present a comparison between the simulated and physical experiments we performed on a real vibratory bowl feeder. We conclude by discussing how simulation can be used to find an optimal configuration of a feeder gate.

2 Related Work

The current design of parts feeders is based primarily on modifications to previous designs and empirical debugging, rather than on theory and automated design. We would like to automate the formal and reliable design of sensorless parts feeders. We use dynamic simulation to address the parts feeder design problem. A number of researchers have investigated this problem and related problems analytically.

Boothroyd and his colleagues, Murch and Poli, developed a taxonomy of industrial parts and corresponding feeders for orienting them. Their work was seminal in examining geometrical and physical considerations of the feeder design problem [3; 14].

The tool we developed previously, enables us to automatically generate and perform many experiments over a parameterized multidimensional space of potential designs [1]. In a similar manner, Brost parameterized an *operation space* of grasping motions for producing a desired outcome. His algorithm incorporated uncertainty to guarantee successful operations. He implemented and tested his planner successfully using a real manipulator [5].

Natarajan introduced several formal paradigms for designing sensorless parts feeders [15]. Erdmann, Mason, and Vaněček developed a sensorless table-tilting planner for orienting three-dimensional polyhedral parts [7]. These two papers, along with the description of the Markov model in our previous work, propose modelling the parts feeding problem using state transitions.

Others have developed analytical methods to uniquely orient singulated parts being fed in a stream. Goldberg described a planning algorithm and automatic programmable parts feeder that can orient parts rapidly by analyzing their geometry [8]. Brokowski, Peshkin, and Goldberg proposed the use of curved fences above a moving conveyor to orient streams of parts [4].

Research in the past few years has included the development of sensorless strategies to manipulate parts using vibratory motion. Böhringer, Bhatt, and Goldberg examined the use of changing dynamic modes of a vibrating plate to orient parts sitting on the plate [2]. Christiansen, Edwards, and Coello Coello developed a genetic algorithm that searches for optimal designs of vibratory bowl feeders [6]. Our system generates the feeder gate probabilities required by their algorithm as input.

More recently, researchers have compared estimates from analytical methods to physical experiments in the industrial parts feeding domain. Mirtich et al. presented a systematic comparison of quasi-static algorithmic and Monte Carlo simulated approaches to physical experiments [13]. Krishnasamy, Jakiela, and Whitney analyzed vibration-assisted entrapment of both simulated and physical experiments [10]. Reznik, Brown, and Canny presented a qualitative examination of micro-actuated motion arrays based on dynamic simulation and physical results [16]. In this paper, we compare simulated and real designs for vibratory parts feeding.

3 Modelling And Experimental Setup

To run physical and simulated vibratory feeding experiments "side-by-side", we developed models of a vibratory bowl feeder and parts by using measurements taken from an actual industrial vibratory bowl and the parts it was designed to orient.

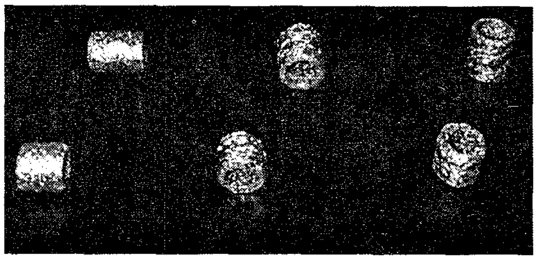

Figure 2: Industrial parts for vibratory feeding and orienting. Medium-sized parts are shown in the foreground and tall-sized parts are shown in the background.

The feeder we used is a vibratory bowl feeder manufactured by *Vibromatic Company, Inc.* (see Figure 1). We used tall- and medium-sized cylindrical parts in our experiments. The actual parts are cylindrical shells or sleeves that are made of stainless steel wire mesh covered with aluminum foil. The *cylindrical sleeves* are actual parts that are used in the automotive industry (see Figure 2).

3.1 Vibratory Motion

A vibratory bowl's oscillating leaf springs cause a constrained motion of torsional vibration about the feeder's vertical axis coupled with translational vibration in its vertical direction.

The resulting motion of parts at any point on the bowl's horizontal track is along a line determined by the bowl's vibration angle ψ and amplitude A. The amplitude controls how big the vibrational motions are, or how much energy is put into the system (see Figure 3).

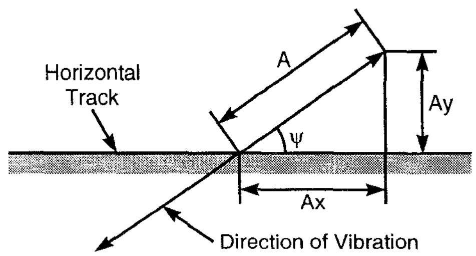

Figure 3: Motion of the track floor in a vibratory bowl, where A_x and A_y are the horizontal and vertical components of the amplitude A, respectively, and ψ is the vibration angle.

When the bowl feeder is operating properly, the vertical component of its amplitude will be the same at every location in the bowl. The horizontal component of vibration varies linearly with the distance from the bowl's axis of rotation.

3.2 Feeder Description

The Vibromatic, Inc. feeder we used to execute our physical experiments is approximately 23 inches high and 32 inches

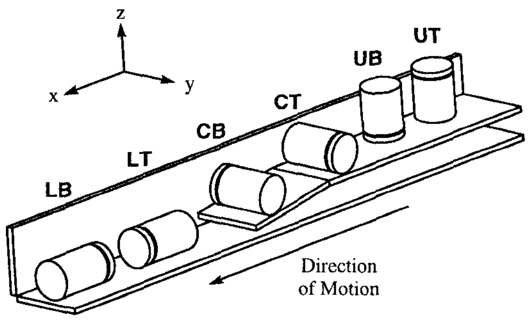

Figure 4: The six cylinder orientations – Upright Top (UT), Upright Bottom (UB), Crosswise Top (CT), Crosswise Bottom (CB), Lengthwise Top (LT), Lengthwise Bottom (LB) – feeding across the Slope gate (figure to scale).

in diameter. It has a mass of about 750 pounds and includes a stainless-steel hopper bowl that weighs about 250 pounds (see Figure 1). A reconfigurable vibratory bowl feeder of this nature and size costs approximately $8500.

The bowl is mounted to a steel base drive unit. Four sets of leaf springs are attached to the base. Two electromagnetic coils attached to the base cause the leaf springs to oscillate at 60 Hertz, delivering 60 vibrational mechanical motions to the bowl per second. The amplitude of these vibrations is adjustable.

The bowl itself has reconfigurable selectors, or *gates*, that are located at various points along the bowl's helical track. The different sections of track preceding and following the gates have varying positive and negative values of pitch. Additionally, the track has varying inward and outward roll. The gates along the track can be easily reconfigured for a number of discrete settings (through the use of thumb-type screws for making the adjustment).

3.3 Part Modelling

We model the cylindrical sleeves as solid, many-faceted cylinders of uniform size and mass. However, the actual cylinders vary in size and mass from part to part. For each cylinder size, we thus modelled the mass, height, and diameter by taking the median of each of the dimensions from a sampling of the bulk parts. In our models the *mid-* and *tall-sized* cylinders have diameters of 3.0 cm, heights of 2.5 and 3.7 cm, and masses of 9 and 12.5 grams, respectively (see Figure 2). We measured the dimensions and masses of the parts manually using rulers and mass balances.

We decomposed the state space of possible stable cylinder orientations into three equivalence classes: *Upright (U)*, *Crosswise (C)*, and *Lengthwise (L)*. However, some parts flip 180 degrees in the course of feeding through the gate, so we found it useful to further subdivide each of these into two classes called *Top (T)* and *Bottom (B)*. To distinguish between the subclasses, we imagine painting a ring around one end of each cylinder. This gives us a total of six classes, labelled UT, UB, CT, CB, LT, and LB, respectively (see Figure 4). To account for radial symmetry about the cylinder's major axis, each equivalence class consists of twelve states formed by rotating the part about its major axis in thirty degree increments.

3.4 Simulated Designs

We model a vibratory bowl feeder as a single straight track formed by unravelling the bowl's helical track. As long as a feeder's gates are far enough apart not to interact, we can study their effects in isolation [14]. Simulating each gate with our tool independently allows us to compute the probability for each pre- and post-orientation of the gate that one will be converted into the other.

Although the actual bowl has several different gates, in this work we simulate and study one particular gate, *Slope* (see Figure 4). Slope can be reconfigured to have various angles of decline. It is designed to turn Lengthwise parts onto their ends, and to allow Upright parts to pass unchanged. At the gate's sub-optimal settings, it reorients few parts into their upright orientations and knocks most upright parts into the lengthwise orientations.

Our simulations model the physical bowl feeder's fixed and varying parameters. Our geometrical model is based on dimension and angle measurements we took of the feeder using rulers and protractors. From these measurements, we approximated the bowl's vibration angle and amplitude, track angle, and gate dimensions. Since determining the vibration amplitude was difficult, we simulated two amplitude values in our experiments.

All the centers of mass and moments of inertia of the objects in the simulations are computed automatically by Impulse, based on the objects' geometrical models.

We referenced a standard chart (which lists friction coefficients for common materials) in a physics text to choose the coefficient of friction. To determine the coefficient of restitution, we attempted to observe the actual part's interaction with the physical feeder. However, since this was somewhat difficult, we also varied restitution over a small range of values in our simulations.

The tool we developed previously enables us to automatically generate and perform many experiments over a multidimensional space of potential designs. It automatically generates the multiple design experiments by taking the Cartesian product over all the parameter values. It also allows us to specify equivalence classes of stable states, and it then automatically categorizes the state (and hence, the equivalence class) of each part as the part exits the gate.

4 Experimental Results

All of the results collected for the physical bowl experiments were observed and recorded by a human observer. For each of the three initial stable orientations, Crosswise (CT), Upright (UT), and Lengthwise (LT), we observed 500 trials of

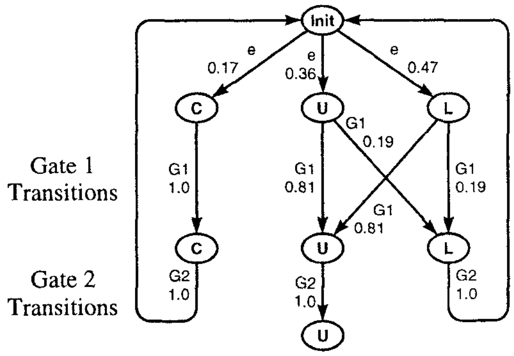

Figure 5: Markov model representing two consecutive gates, Slope and Discharge Chute (labelled G1 and G2), in our simulated vibratory bowl feeder for the mid-sized cylinders. Gate 1 was simulated with Slope = 12.8°, Amplitude = 0.06 cm, and Restitution = 0.4. The epsilon (e) probabilities and the Gate 2 probabilities were taken from the actual feeder data.

singulated (non-interacting) parts moving across the Slope gate. We observed physical experiments for each of the two-sized parts with the angle of Slope set to 12.8 degrees and a measured vibration angle of 15 degrees (see Figure 3).

For the simulations, we varied the feeder's coefficient of restitution and vibration amplitude. In particular, we experimented with restitution values ranging over the interval $[0.3, 0.5]$ in step sizes of 0.1, and we examined vibration amplitudes of 0.06 and 0.1 cm. Each experiment consisted of a suite of 500 trials for a fixed set of parameter values for each of the three initial part orientations.

4.1 Markov Model Development

We represent the effects produced by the feeder's gates as state transitions in a non-deterministic finite state automaton (NFA). In our experiments the states are the stable cylinder orientations that we enumerated earlier (see Figure 4).

We use our tool to compute the probability that a part in a particular initial orientation will end up in each final orientation as it passes through a gate. We thus use our simulation results from Impulse to generate Boothroyd's stochastic matrices [14]. We can also attach the gate probabilities derived from our experimentation to the edges or state transitions of the NFA. Both Boothroyd's model and the NFA model allow us to compute transition probabilities for the entire feeder.

Figure 5 shows a Markov model representation of the feeder. The feeder in this figure consists of Slope, the first gate (labelled G1), and the final gate, *Discharge Chute* (labelled G2), through which correctly or incorrectly oriented parts will pass or be recycled, respectively.

The transitions out of the initial state, *Init*, (labelled *e* for epsilon) show that 17%, 36%, and 47% of the cylinders will encounter the first gate while in the Crosswise (C), Upright (U), or Lengthwise (L) orientations, respectively. These probabilities were obtained from physical experimentation.

Simulated Transition Probabilities (%)

Initial State	Final State: UT	UB	LT	LB	CT	CB
Upright (UT)	4.2	**56.8**	**34.6**	1.6	0.0	2.8
Lengthwise (LT)	**62.4**	3.2	**22.4**	**10.4**	1.0	0.6
Crosswise (CT)	0.0	3.6	3.6	4.4	0.2	**88.2**

Figure 6: Probability matrix for simulation of mid-sized cylinders with Slope = 12.8°, Amplitude = 0.10 cm, and Restitution = 0.4 (significant probabilities are highlighted in boldface).

Actual Transition Probabilities (%)

Initial State	Final State: UT	UB	LT	LB	CT	CB
Upright (UT)	1.6	**47.4**	**30.8**	0.2	0.0	**20.0**
Lengthwise (LT)	**84.2**	0.4	**13.4**	1.4	0.4	0.2
Crosswise (CT)	0.6	0.0	0.0	3.2	0.6	**95.6**

Figure 7: Probability matrix for actual feeding of mid-sized cylinders with Slope = 12.8° (significant probabilities are highlighted in boldface).

The G1 edges in figure represent the feeder's state transitions and associated probabilities obtained from one of the simulations. The representation shows that for this experiment, Slope always leaves Crosswise cylinders unchanged, and for the most part, does not reorient Upright cylinders. But it inverts Lengthwise cylinders into the Upright orientation most of the time.

Figure 6 conveys the same type of information in a slightly different form, using Boothroyd's stochastic matrix representation. This figure gives results for another mid-sized cylinder simulation, one in which the amplitude was higher. Figure 7 gives the matrix for the corresponding physical experiment.

4.2 Stochastic Matrices

Figures 6 and 7 show results for three simulated and actual mid-sized cylinder experiments performed on the single Slope gate. Each row in the matrix represents 500 trials, each for a feeder amplitude of 0.10 cm and a coefficient of restitution of 0.4.

The figures show that our simulated experiments gave similar results to the physical ones. As highlighted by the bold entries, the relative error between the matrices is small. However, we also note a couple of marked differences. For example, the simulated feeder has a much higher relative probability of rotating the lengthwise parts 180 degrees to the LB orientation than does the physical feeder. We can also see by comparing the matrices that the actual gate is more likely to turn Upright parts into the Crosswise orientation.

These differences may be due to more randomness in the physical world than what we have modelled in our simulations. Since Impulse is deterministic, we perturb the initial orientation of the cylinder in each trial slightly to introduce some randomness into our simulated experiments. However, we may still need to consider other uncertainties in the real world.

4.3 Simulated vs. Physical Designs

To gain a broader perspective on the similarities and differences between the two types of design experiments for the Slope gate, we compared the complete data distributions.

Figure 8 shows the outcome orientations for the mid-sized cylinder, beginning in the Lengthwise, Upright and Crosswise attitudes. The figure shows similar trends in the real and simulated data. In particular, if we rank order the outcome percentages for each experiment, the orders of the simulated and physical experiments agree for the top three outcomes. These are the most significant, since they account for over 95% of the outcomes. For example, when the parts are initially Lengthwise, the rank order of the actual outcomes is UT, LT, and LB. These account for 99% of the outcomes. For each of the six simulations, the top three outcomes in rank order are the same.

There are some notable exceptions to the similarities between the actual and simulated experiments. When the parts are initially Upright, 20% of the actual cylinders end up in the Crosswise orientation. However, less than 5% of the parts in the simulated experiments finished in that orientation. This may be due to the differences between the actual part and our model of it. The actual cylindrical sleeve has rounded edges and is somewhat deformable, unlike the simulated part. These differences may tend to cause it to roll into other orientations when it begins in the Upright orientation.

What is the correlation between the simulated feeder parameters and the physical accuracy of the simulated experiments? It is clear that both the vibration amplitude and the coefficient of restitution are significant factors in the simulated experiments. However, there is no one set of values for these parameters that best correlate with reality. One source of simulation inaccuracy may be due to our modelling of the physical world. Another may be due to limitations in the way Impulse models collisions between vibrational parts. We are currently investigating these possibilities.

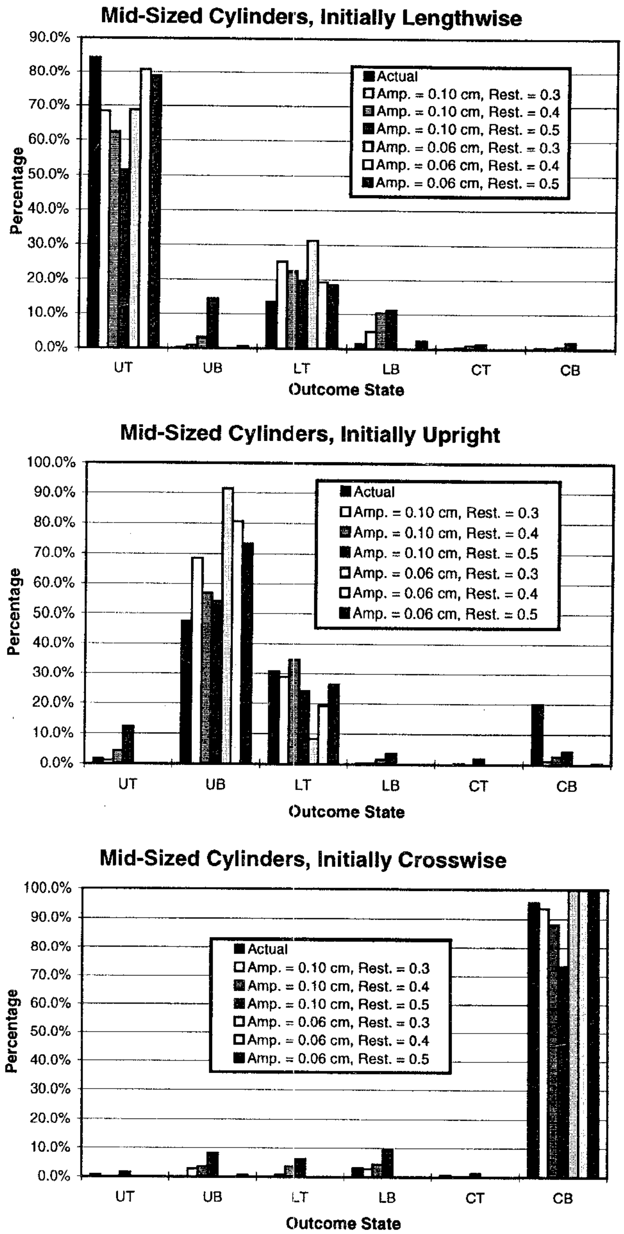

Figure 8: Actual vs. simulated probabilities of six outcome states for parts starting in the Lengthwise (LT), Upright (UT), and Crosswise (CT) orientations. The angle of the Slope gate was 12.8° for these experiments.

4.4 Finding An Optimal Configuration

We are interested in learning whether Impulse can find an optimal configuration for the gate in the actual bowl. To do this, we studied the tall cylinders for varying Slope angles. We ran simulated and physical trials of 350 parts, with Slope angles varying over the interval [-2.3, 17.0] (the physical gate's lower and upper angle bounds), in steps of 5.5 degrees, and restitution values of 0.4 and 0.5.

Figure 9 shows the probability that a part in the Lengthwise (LT) orientation will land in each of the UB, LT, and LB orientations for various combinations of Slope angles and restitution values. As before, the rank ordering of the simulated and physical outcomes is identical. We also see that the difference between actual and simulated experiments, where Slope is 6.0 and 17.0 degrees, is small; the experiments for angles of 0.5 and 11.5 differ more substantially in the worst case.

Our simulations indicate that cylinders are most likely to fall onto their ends from the Lengthwise orientation when the Slope angle is 0.5 degrees; that probability is lowest when the Slope angle is 17.0 degrees. The probabilities for Slope angles between 0.5 and 17.0 degrees decrease as the

Slope	Experiment	Final State UB	LT	LB
17.0°	Actual	0.02	0.98	0.00
	Simulated, Rest.=0.5	0.01	0.99	0.00
	Simulated, Rest.=0.4	0.00	1.00	0.00
11.5°	Actual	0.23	0.77	0.00
	Simulated, Rest.=0.5	0.19	0.81	0.00
	Simulated, Rest.=0.4	0.11	0.89	0.00
6.0°	Actual	0.57	0.43	0.00
	Simulated, Rest.=0.5	0.54	0.46	0.00
	Simulated, Rest.=0.4	0.55	0.45	0.00
0.5°	Actual	0.87	0.09	0.04
	Simulated, Rest.=0.5	0.69	0.25	0.05
	Simulated, Rest.=0.4	0.72	0.27	0.01

Figure 9: A comparison of actual and simulated outcomes for various slope angles when the cylinder starts in the Lengthwise (LT) Orientation. The vibration amplitude in these experiments was 0.06 cm.

angle increases. Interestingly enough, our simulations also show that at a Slope angle of -2.3 degrees (not shown in the figure), the probabilities fall off again. This may indicate some type of wrap-around behavior in the space of designs. We would like to investigate this possibility further.

5 Conclusions

Dynamic simulation is a potentially powerful alternative to the time-consuming and costly trial-and-error technique currently used in industry to design industrial parts feeders. However, in order for dynamic simulation to be effective, it must accurately predict the behavior of real parts feeders. In this paper, we have measured a real industrial vibratory bowl feeder and modelled it using dynamic simulation. Our simulation results correlate well with reality. However, there are still some differences that we are currently investigating. Despite these differences, we continue to believe that dynamic simulation holds promise as a rapid and effective technique for designing parts feeders.

Acknowledgments

Much thanks to Doug Daubenspeck and Vibromatic Company, Inc. for their generous donation of a vibratory bowl feeder to our lab for this work. The authors would also like to thank Allan Heydon and Greg Nelson for help with their constraint-based drawing editor, Juno-2, which was used to draw Figures 3, 4, and 5 [9].

References

[1] Dina R. Berkowitz and John Canny. Designing parts feeders using dynamic simulation. In *International Conference on Robotics and Automation*. IEEE, April 1996.

[2] Karl-Friedrich Böhringer, Vivek Bhatt, and Kenneth Y. Goldberg. Sensorless manipulation using transverse vibrations of a plate. In *International Conference on Robotics and Automation*. IEEE, May 1995.

[3] Geoffrey Boothroyd, Corrado R. Poli, and Laurence E. Murch. *Handbook of Feeding and Orienting Techniques for Small Parts*. Department of Mechanical Engineering, University of Massachusetts, Amherst, MA, 1976.

[4] Mike Brokowski, Michael A. Peshkin, and Ken Goldberg. Curved fences for part alignment. In *International Conference on Robotics and Automation*. IEEE, May 1993.

[5] Randy C. Brost. Automatic grasp planning in the presence of uncertainty. *International Journal of Robotics Research*, 7(1):4–17, February 1988. Also appeared in Proceedings of the IEEE International Conference on Robotics and Automation, April 1986.

[6] Alan D. Christiansen, Andrea D. Edwards, and Carlos A. Coello Coello. Automated design of part feeders using a genetic algorithm. In *International Conference on Robotics and Automation*. IEEE, April 1996.

[7] Michael Erdmann, Matthew T. Mason, and George Vaněček Jr. Mechanical parts orienting: The case of a polyhedron on a table. *Algorithmica*, 10:226–247, August 1993.

[8] Kenneth Y. Goldberg. Orienting polygonal parts without sensors. *Algorithmica*, 10:201–225, August 1993.

[9] Allan Heydon and Greg Nelson. The Juno-2 constraint-based drawing editor. Research Report 131a, Digital Systems Research Center, December 1994. See http://www.research.digital.com/SRC/juno-2.

[10] Jayaraman Krishnasamy, Mark J. Jakiela, and Daniel E. Whitney. Mechanics of vibration-assisted entrapment with application to design. In *International Conference on Robotics and Automation*. IEEE, April 1996.

[11] Brian Mirtich and John Canny. Impulse-based dynamic simulation. In K. Goldberg, D. Halperin, J.C. Latombe, and R. Wilson, editors, *The Algorithmic Foundations of Robotics*. A. K. Peters, Boston, MA, 1995. Proceedings from the workshop held in February, 1994.

[12] Brian Mirtich and John Canny. Impulse-based simulation of rigid bodies. In *Symposium on Interactive 3D Graphics*, New York, 1995. ACM Press.

[13] Brian Mirtich, Ken Goldberg, Yan Zhuang, John Craig, Rob Zanutta, Brian Carlisle, and John Canny. Estimating pose statistics for robotic part feeders. In *International Conference on Robotics and Automation*. IEEE, April 1996.

[14] L. E. Murch and G. Boothroyd. Predicting efficiency of parts orienting systems. *Automation*, 18, February 1971.

[15] Balas K. Natarajan. Some paradigms for the automated design of parts feeders. *International Journal of Robotics Research*, 8(6):98–109, December 1989. Also appeared in Proceedings of the 27th Annual Symposium on Foundations of Computer Science, 1986.

[16] Dan S. Reznik, Stan W. Brown, and John Canny. Dynamic simulation as a design tool for a microactuator array. In *International Conference on Robotics and Automation*. IEEE, April 1997.